Electronic Supplementary Information

Crumpled N-doped Carbon Nanotubes Encapsulated with Peapod-like Ge Nanoparticles for High-rate and Long-life Li-ion Battery Anodes

Kaifu Huo, [a,*] *Lei Wang,* [a] *Chanjian Peng,* [a] *Xiang Peng,* [b] *Yuanyuan Li,* [a] *Qingwei Li,* [a] *Zhenzhen Jin* [c] *and Paul K Chu*[b]

[a] Wuhan National Laboratory for Optoelectronics(WNLO), Huazhong University of Science and Technology, Wuhan 430074, P. R. China

[b] Department of Materials Science and Physics, City University of Hong Kong, Tat Chee Avenue, Kowloon, Hong Kong, P. R. China

[c] School of chemistry and chemical engineering, Huazhong University of Science and Technology,Wuhan 430074, P. R. China

Contents:

Experimental details

Fig.S1-Fig.S14

Table S1

Experimental details

Synthesis of Inorganic-organic hybrid GeO_x/EDA nanowires

GeO_x/EDA nanowires were prepared by a facile and low-cost solvothermal process.[1, 2] In a typical procedure, 1 g GeO_2 and 0.25 g Fe_2O_3 were mixed together and then transferred to a 50 ml Teflon-lined stainless-steel autoclave filled with 8 ml H_2O and 5 ml EDA. After hydrothermal treatment at 200 ^oC for 60 h, the products were collected, then thoroughly washed with ethanol for three times, and finally vacuum dried at 60 ^oC for 3 h.

Synthesis of 1D peapod-like Ge/CN_x nanomaterials

The as-synthesized GeO_x/EDA nanowires were annealed in the air at 500 ^oC for 2 h to remove the EDA. The as-synthesized GeO_2 nanowires were further coated with polypyrrole (PPy) and then thermally treated under Ar/H_2 at 850 ^oC to produce peapod-like Ge/CN_x nanomaterials. In a typical synthesis, 300 mg GeO_2 nanowires was firstly dispersed in anhydrous methylacetate (20 mL) containing 100 mg anhydrous $FeCl_3$ as an oxidant and 20 mg poly(vinyl acetate as a stabilizing agent. Then monomer pyrrole (20 μL; 0.97 mg/μL) was added dropwise. After stirring for overnight reaction at room temperature, the PPy coated GeO_2 nanowires were collected and washed three times with methyl acetate. After vacuum dried at 60 ^oC overnight, the GeO_2@PPy nanowires were thermally treated in a tube furnace under Ar/H_2 atmosphere (10% H_2) at 850 ^oC for 2 h with the heating ramp of 5 ^oC min^{-1}.

Structural and Electrochemical Characterizations

The morphology, structures and composition of samples were characterized by X-ray diffraction (GAXRD, Philips X'Pert Pro), field-emission scanning electron microscopy (FE-SEM, FEI nanoSEM 450), transmission electron microscopy (TEM, FEI Titan 60-300Cs), high-resolution

TEM (HR-TEM, JEM-2010F) and energy-dispersive X-ray spectroscopy (EDS, Oxford INCA 200, Oxford Instruments, and Oxfordshire, U.K.). XRD were measured using a Philips X' Pert Pro diffractometer with copper Kα (λ = 1.5416 Å) radiation. X-ray photoelectron spectroscopy (XPS) measurements were conducted on aKratos Axis Ultra DLD spectrometer using a monochromated Al Kα radiation. Raman scattering measurement was measured in LabRam HR with Ar+ laser excitation in back scattering geometry (514.5 nm). The TG results were obtained via TGA (NETZSCH; TG 209 F3) measurements.

The Li storage properties of Ge/CN_x peapods are investigated in the half cell in an electrolyte consisting of 1:1 vol/vol mixture of ethylene carbonate (EC) and diethyl carbonate (DEC) with 5 wt.% Fluorinated ethylene carbonate (FEC). To prepare working electrodes, peapod-like Ge/CN_x, poly(vinyl difluoride) (PVDF, Sigma Aldrich) and carbon black (conducting agent) with the ratio of 80:10:10 were mixed in N-Methyl pyrrolidone (NMP, Sigma Aldrich) forming a slurry and then pasted on a copper foil. The mass loading of Ge active materials is typically about 1.5 mg/cm^2. A Celgard 2400 film was used as the separator and pure Li foil as the counter electrode. The 2025 coin-like cells were assembled in an argon-filled glove box. The charge and discharge measurements of the batteries were conducted with an MTI automatic battery cycler with the voltage cutoffs between 0.01 and 1.5 V *vs* Li/Li^+. The electrochemical impedance spectroscopy (EIS) tested was carried out on Autolab Electrochemical workstation from 10 mHz to 10^5 Hz.

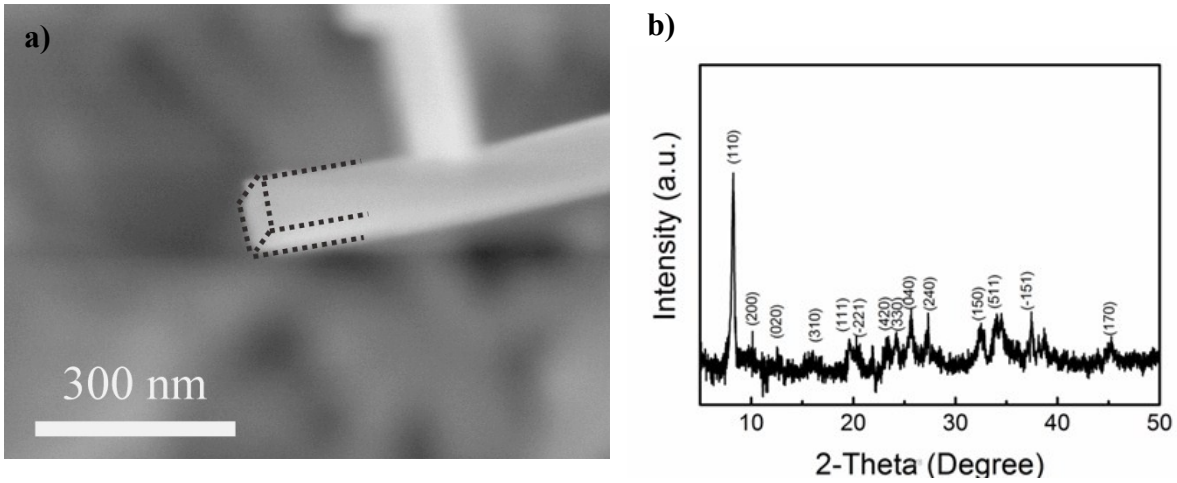

Figure S1. FESEM image (a) and the corresponding XRD pattern (b) of a single inorganic-organic hybrid GeO_x/EDA nanowires with rectangular cross section. The XRD pattern in Fig. S1b is the same as the one acquired from previously-reported GeO_x/EDA, [1,2] suggesting the as-synthesized nanowires are hybrid GeO_x/EDA nanowires.

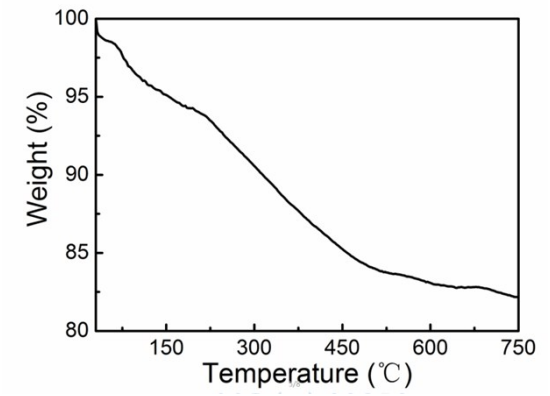

Figure S2. TG curve of inorganic-organic hybrid GeO_x/EDA nanowires under Air.

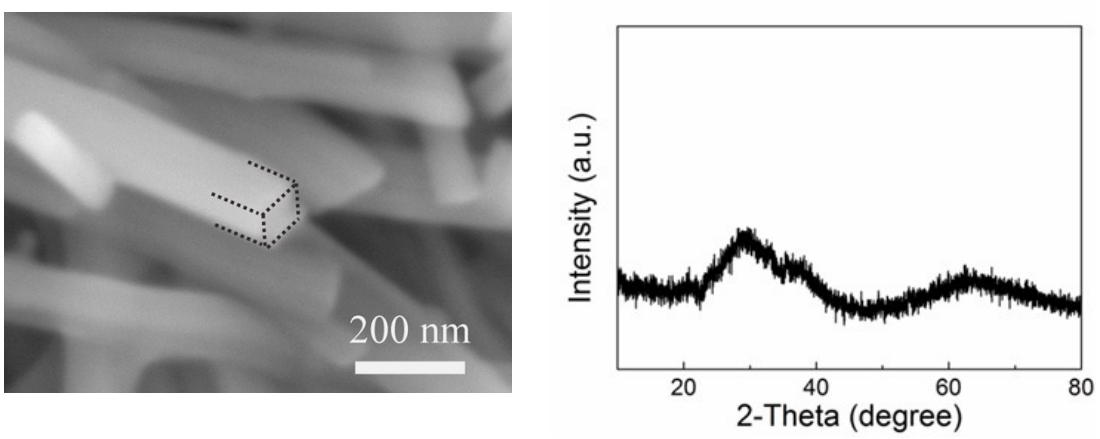

Figure S3. FESEM image and corresponding XRD pattern of GeO_2 nanowires.

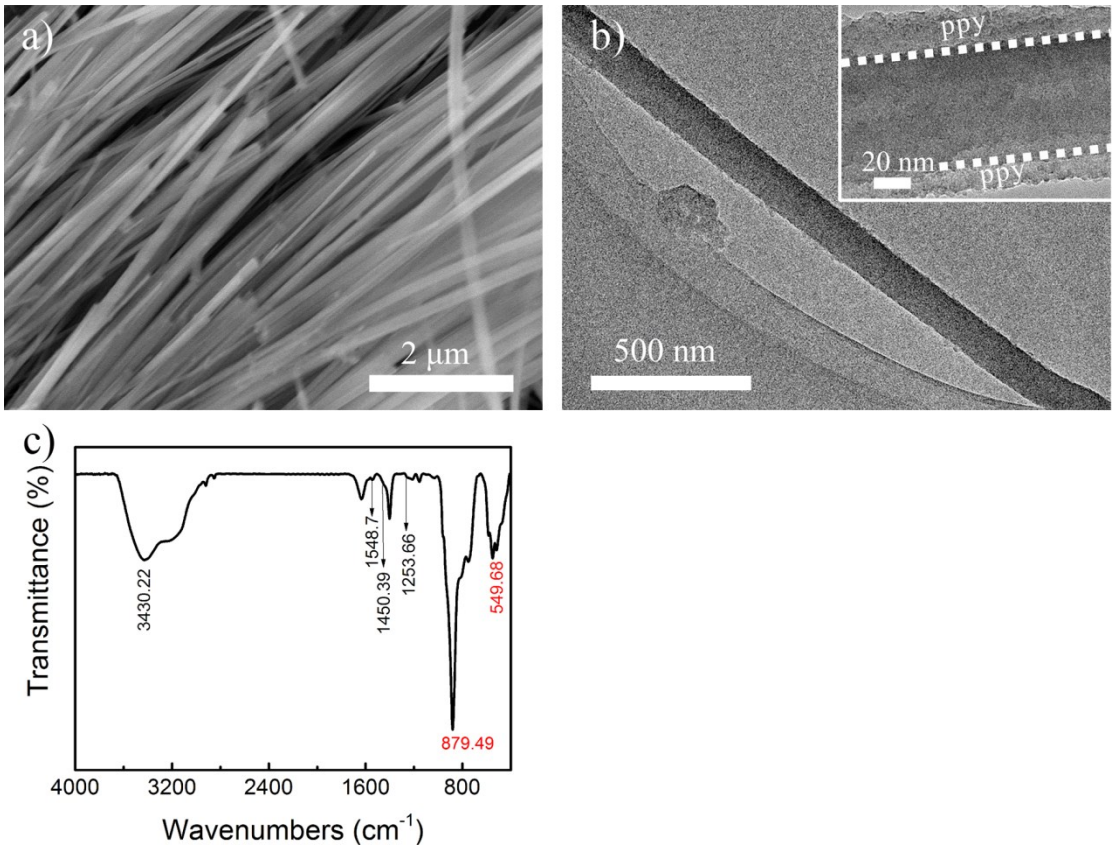

Figure S4. FE-SEM (a), TEM (b) and FTIR spectrum (c) of PPy coated GeO_2 nanowires. The thickness of PPy shell is about 15-20 nm. In Figure c, the IR absorption peaks centered at 549.6 and 874.9 cm^{-1} band indicate the existence of GeO_2 and the peaks at 3430.2, 1548.7, 1450.4 and 1253.7 cm^{-1} confirm the presence of PPy shell.

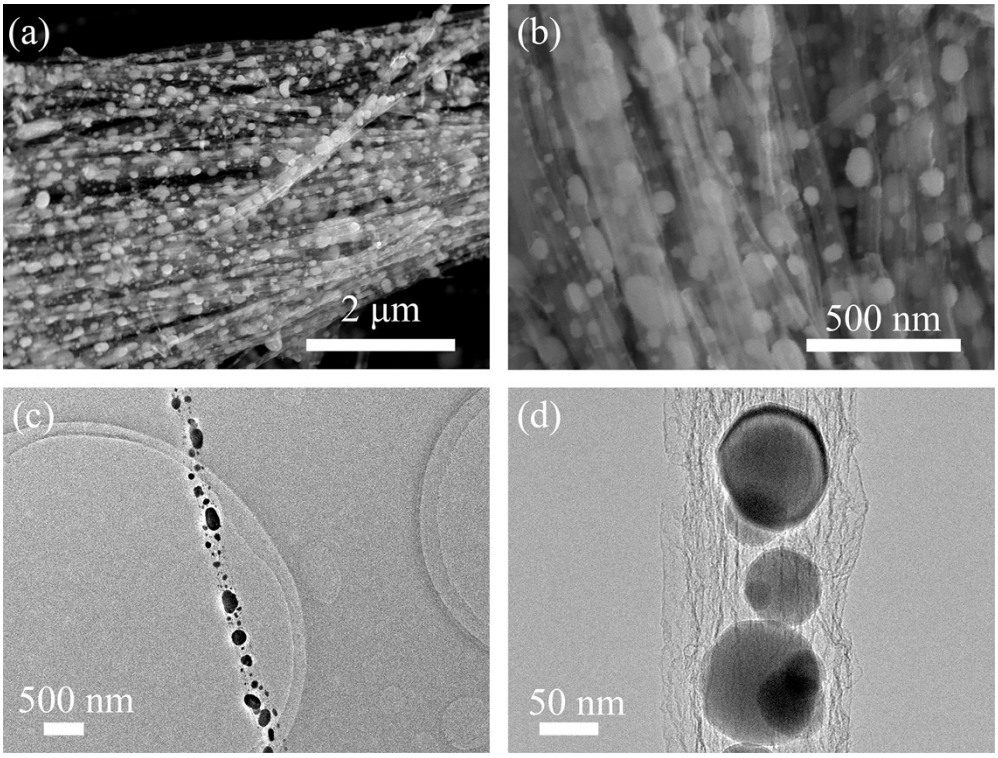

Figure S5. Different magnified SEM (a, b) and TEM(c, d) images for Ge/CN_x nanopeapods, confirming that the isolated NPs are incorporated into the nanotubular shells resembling peapods.

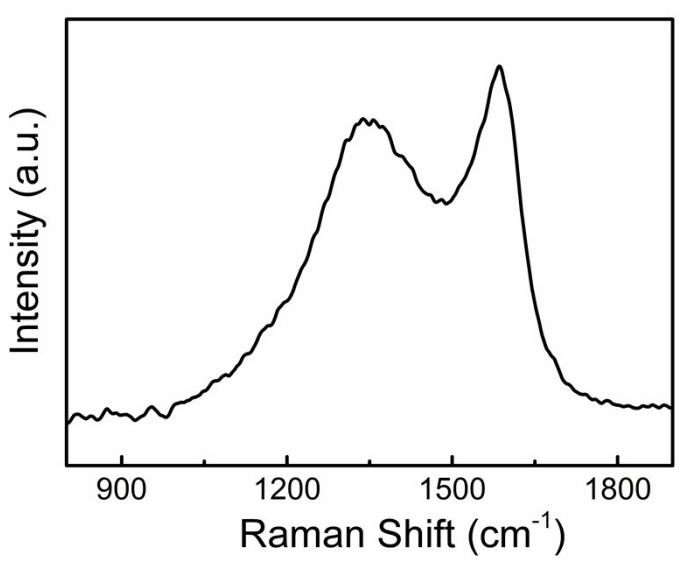

Figure S6. Raman Spectrum of Ge/CN_x in the range of 800-1900 cm^{-1}.

Different from the Raman spectrum of carbon nanotubes with two distinct D and G bands, [3-4] Raman scattering spectrum in Fig. 2c demonstrates a dramatic broadening and overlap of D (1350) and G (1850 cm^{-1}) bands for CN_x shell. The peak

at G-band is attributed to the vibration of sp^2-bonded carbon atoms in a 2D hexagonal lattice, namely, the stretching modes of C-C bonds of typical graphite, while the peak at D-band is associated with vibrations of carbon atoms with dangling bonds in plane terminations of the disordered graphite and is related to the defects and disorders of structures in carbon materials. The presence of N in the CN_x shell result in an asymmetric tailing of D band extending out to about 1000 cm^{-1} as well as two broadening and overlap of D and G bands. In our case, the I_D/I_G in the Raman scattering spectrum is estimated to be ~0.95, meaning that the CN_x nanotubes is partially graphitized, which is in accordance with previous reported results. [3-5]

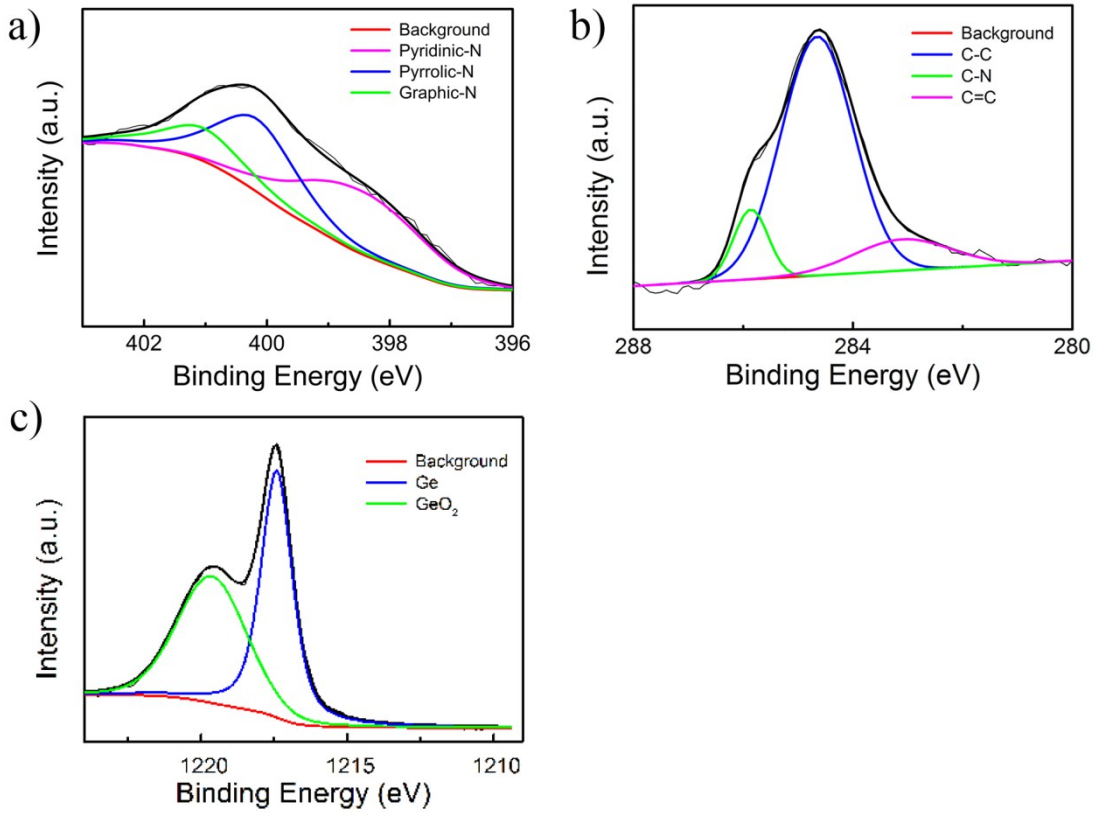

Figure S7. The X-ray photoelectron spectroscopy (XPS) results of Ge/CN_x nanopeapods. (a) The high-resolution N 1s spectrum can be deconvoluted into pyridinic N (398.2 eV), pyrrolic N (400.1 eV), and graphitic N (401.1 eV);(b) Fine XPS of C 1s; (c) The fine XPS of Ge 2p shows an intense peak at 1217.4 and weak peak at 1219.8 eV, corresponding to the Ge and GeO_2, respectively.

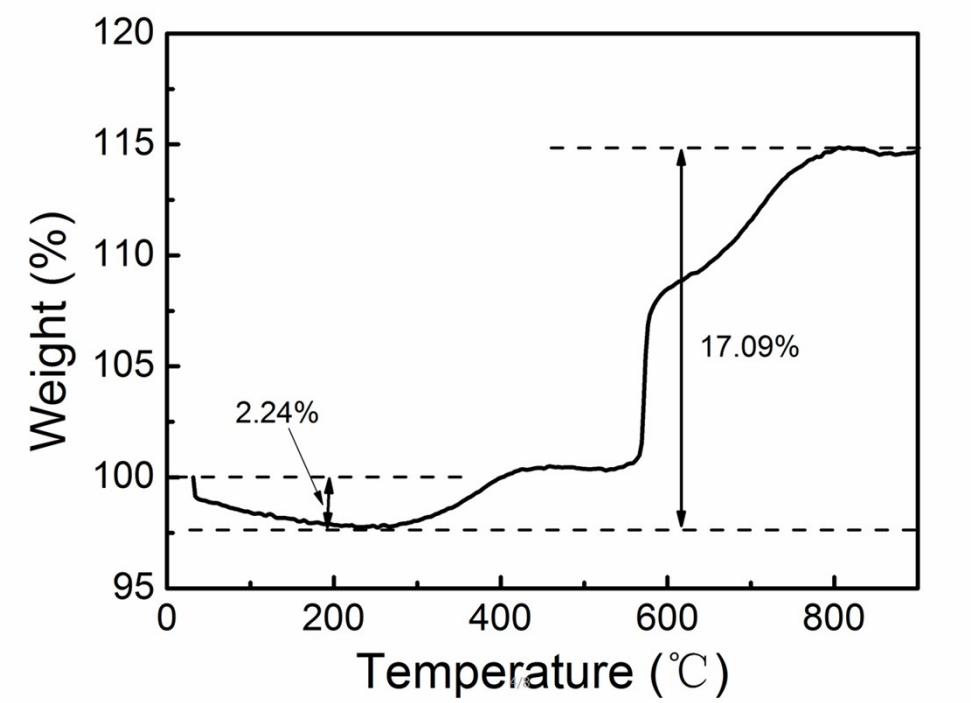

Figure S8. TG profile for peapod-like Ge/CN_x. Assuming the Ge was fully transformed into GeO_2, the weight ratio of CN_x in Ge/CN_x peapods is calculated to be 18.2 %.

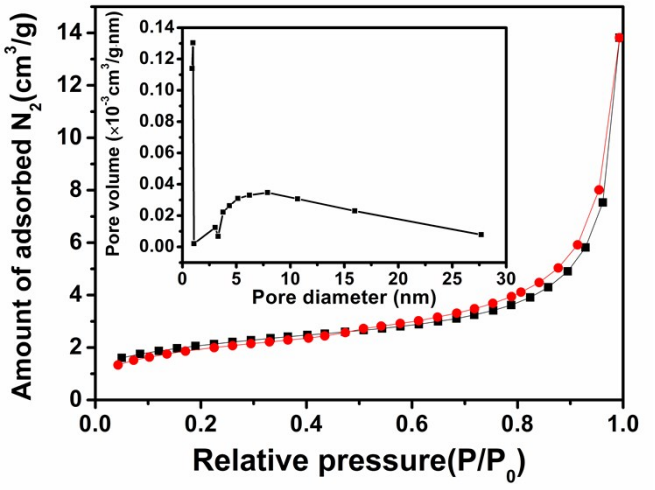

Figure S9. Nitrogen adsorption-desorption isotherms and pore distribution of peapod-like Ge/CN_x. The measured BET surface area is about 19.5 m^2 g^{-1}.

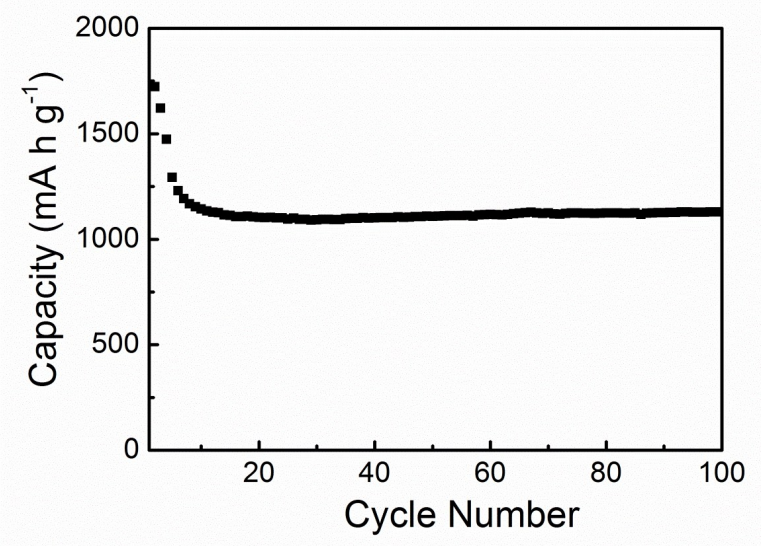

Figure S10. Delithiation capacity of the Ge/CN_x nanopeapods as a function of cycle numbers based on the mass loading of Ge active materials, revealing that the capacity is as high as 1200 mA h g^{-1} after initial 5 cycles at a 0.5 C rate.

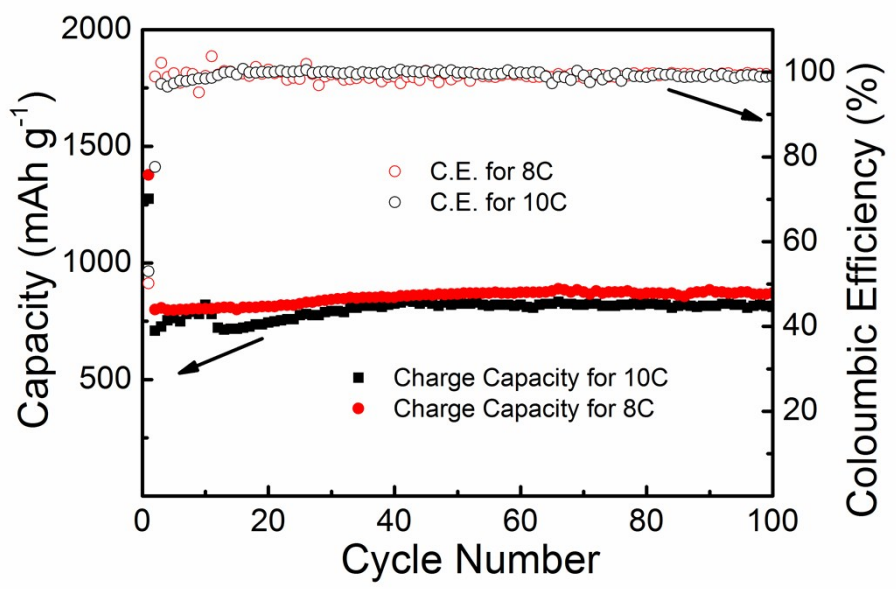

Fig. S11. Cycling performance of Ge/CN_x nanopeapods at high rates of 8 and 10 C. The reversible capacity at a 10 C rate is measured to be about 810 mA h g^{-1}.

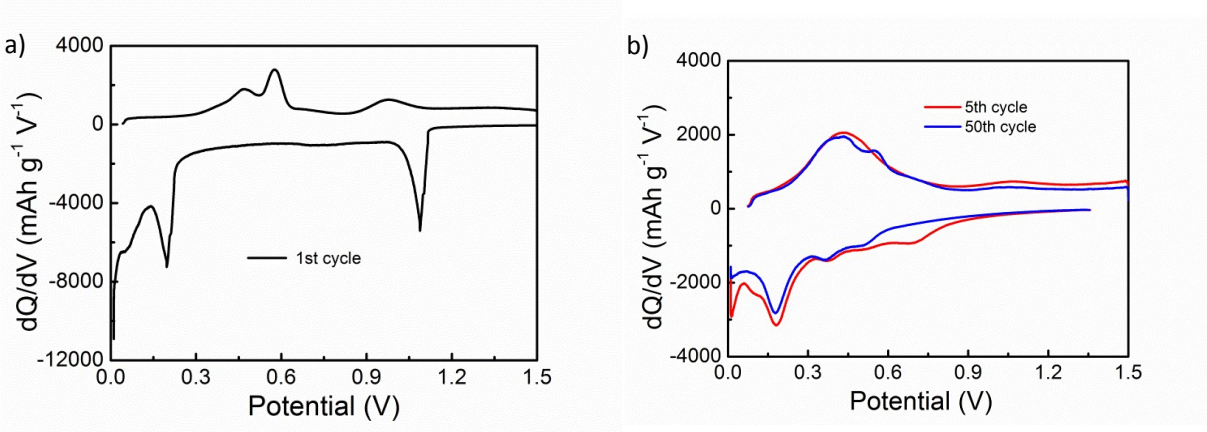

Figure S12. The differential plots (dQ/dV *vs*. V) for the 1st, 5th and 50th cycles. The three peaks at 0.17, 0.36, and 0.49 V are related to the different Li_xGe alloys formed during lithiation. The peaks between 0.3 and 0.7 V in the oxidation scan can be ascribed to delithiation of Li_xGe.

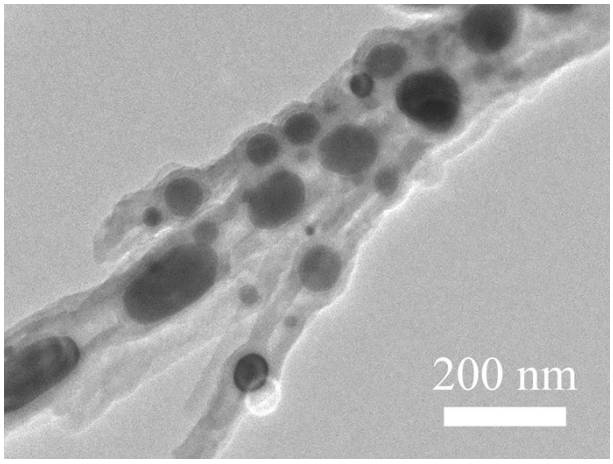

Figure S13. Low-magnification TEM image of the Ge/CN_x nanopeapods after 1200 cycles

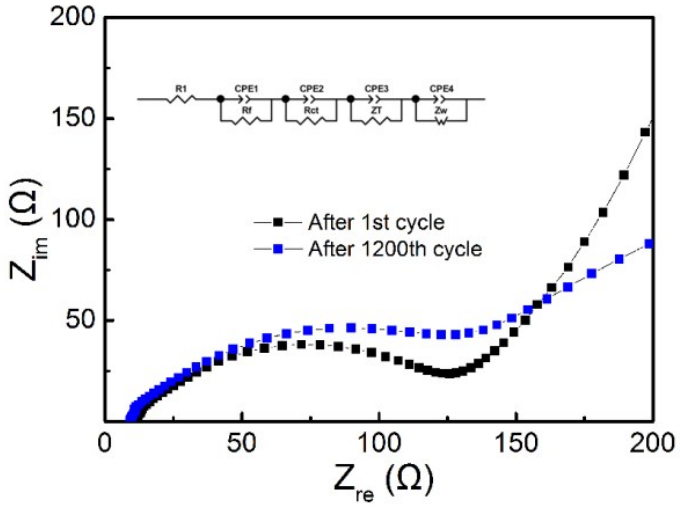

Figure S14. The EIS results of the Ge/CN_x after the 1st and 1200th cycle and the corresponding equivalent circuit. The semicircle at high frequencies can be assigned to the SEI resistance and contact resistance (R_f) and the charge transfer impedance on electrode−electrolyte interface (R_{ct}). After 1200th cycle, the R_f slightly enlarges from 101 to 119 Ω while the R_{ct} decreases from 98 to 30 Ω, suggesting stable SEI and structural stability of Ge/CN_x for the continuous cycles.

Table S1. Comparison of electrochemical performance found in the present work with those of reported Ge-based materials.

Sample	**Cycle Stability**	**Rate performance**	R_{ct} (Ω)	**Ref.**
C-N/Ge	906. $mAhg^{-1}$@50 cycles@600 mAg^{-1}	500 mAh g^{-1}@4A g^{-1}		6
Ge/RGO/C	993 mAh/g@600cycles@1000 mAg^{-1}	750 $mAhg^{-1}$@9.6A g^{-1}		7
Ge@C-N	813 mAh g^{-1}@90cycles@500 mA g^{-1}	406 $mAhg^{-1}$@3A g^{-1}	23.3	8
Ge@C	328.6mAh g^{-1}@90cycles@500 mA g^{-1}	200 $mAhg^{-1}$@3A g^{-1}	45.7	8
P-Ge@C	1099mAh g^{-1}@100cycles@160mA g^{-1}	708 mA h g^{-1}@1.6A g^{-1}	78	9
Ge-C	900$mAhg^{-1}$@50cycles@150mA g^{-1}	613 mAh g^{-1}@0.9Ag^{-1}		10
Pc-Ge NWs	789$mAhg^{-1}$@50cycles@160mA g^{-1}	450 mAh g^{-1}@1.6Ag^{-1}		11
Ge/N-RGO	700$mAhg^{-1}$@200cycles@500mA g^{-1}	210 mAh g^{-1}@10Ag^{-1}	12.1	12
Hollow Ge@C	1137 mA h g^{-1}@200cycles@320mAg^{-1}	360 mAh g^{-1}@40Ag^{-1}		13
Ge–MWCNT	800 mA h g^{-1}@200cycles@320mAg^{-1}	490 mAh g^{-1}@8.115Ag^{-1}		14
Ge-CN_x nanopeapods	1080$mAhg^{-1}$@1200cycles@800 mAg^{-1}	874 mA h g^{-1}@12.8Ag^{-1}	30	This work

References

1. Q. S. Gao, P. Chen, Y. H. Zhang and Y. Tang, *Adv. Mater.*, 2008, **20**, 1837-1842.
2. J. Liu, K. P. Song, C. B. Zhu, C. C. Chen, P. A. van Aken, J. Maier and Y. Yu, *Acs Nano*, 2014, **8**, 7051-7059.
3. S. Maldonado, S. Morin and K. J. Stevenson, *Carbon*, 2006, **44**, 1429-1437.
4. L. G. Bulusheva, A. V. Okotrub, I. A. Kinloch, I. P. Asanov, A. G. Kurenya, A. G. Kudashov, X. Chen and H. Song, *Phys. Status Solidi. B*, 2008, **245**, 1971-1974.

5. F. B. Su, C. K. Poh, J. S. Chen, G. W. Xu, D. Wang, Q. Li, J. Y. Lin and X. W. Lou, *Energy Environ. Sci.*, 2011, **4**, 717-724.

6. Y. Xiao and M. Cao, *Chem- Asian J.*, 2014, **9**, 2859-2865.

7. F. W. Yuan and H. Y. Tuan, *Chem. Mater.*, 2014, **26**, 2172-2179.

8. Y. Xiao and M. H. Cao, *Acs Appl. Mater. Interfaces*, 2014, **6**, 12922-12930.

9. M. X. Liu, X. M. Ma, L. H. Gan, Z. J. Xu, D. Z. Zhu and L. W. Chen, *J. Mater. Chem. A*, 2014, **2**, 17107-17114.

10. G. L. Cui, L. Gu, L. J. Zhi, N. Kaskhedikar, P. A. van Aken, K. Mullen and J. Maier, *Adv. Mater.*, 2008, **20**, 3079-3083.

11. L. P. Tan, Z. Lu, H. T. Tan, J. Zhu, X. Rui, Q. Yan and H. H. Hng, *J. Power Sources*, 2012, **206**, 253-258.

12. Y. Xu, X. Zhu, X. Zhou, X. Liu, Y. Liu, Z. Dai and J. Bao, *J. Phys. Chem. C*, 2014, **118**, 28502-28508.

13. L. Li, K. H. Seng, C. Q. Feng, H. K. Liu and Z. P. Guo, *J. Mater. Chem. A*, 2013, **1**, 7666-7672.

14. I. S. Hwang, J. C. Kim, S. D. Seo, S. Lee, J. H. Lee and D. W. Kim, *Chem. Commun.*, 2012, **48**, 7061-7063.